Springer

Chinese Society of Pavement Engineering

International Journal of
Pavement Research and Technology

Journal homepage: www.springer.com/42947

Numerical analysis of longitudinal cracking in widened jointed plain concrete pavement systems

Orhan Kaya[a]*, Yang Zhang[a], Halil Ceylan[a,b,c], Sunghwan Kim[c], Shuo Yang[a], Peter C. Taylor[d], Kasthurirangan Gopalakrishnan[a,e]

[a]*Department of Civil, Construction and Environmental Engineering (CCEE), Iowa State University, Ames, IA 50011-1066*
[b]*Federal Aviation Administration (FAA) Partnership to Enhance General Aviation Safety, Accessibility and Sustainability (PEGASAS) Center of Excellence (COE)*
[c]*Program for Sustainable Pavement Engineering and Research (PROSPER), Institute for Transportation, CCEE, Iowa State University, Ames, IA 50011-1066*
[d]*National Concrete Pavement Technology Center, Iowa State University, Ames, IA 50010-8664*
[e]*Research, School of Engineering & Applied Sciences (SEAS), SRM University-AP, Amaravati 522 502, India*

Received 19 March 2019; received in revised form 15 April 2019; accepted 17 April 2019

Abstract

While widened slabs have been used to mitigate transverse cracking in jointed plain concrete pavements (JPCP), it is well-known that use of such slabs increases longitudinal cracking potential in JPCP. Field investigations have been conducted in Iowa widened JPCP and it was found that: (1) all longitudinal cracks are top-down cracks; (2) longitudinal cracks start mostly from transverse joints about 0.6-1.2 m (2-4 ft) away from widened slab edges (3) sites with a tied PCC shoulder exhibited fewer longitudinal cracks than sites constructed with hot mix asphalt (HMA) shoulders. In this paper, the longitudinal cracking mechanism of widened JPCP was demonstrated and longitudinal cracking potential was evaluated using numerical analysis. The critical load configuration with the highest longitudinal cracking potential for widened JPCP was identified. Three shoulder design alternatives were also compared in terms of their contributions to mitigation of longitudinal cracking potential. Compared to the use of a widened slab, the use of a regular size slab was found to be beneficial in mitigating longitudinal cracking at the cost of increasing transverse cracking potential. The findings of this study provide explanations as to where and how longitudinal cracking is likely to be initiated as well as recommendations as to how longitudinal cracking potential could be mitigated.

Keywords: Longitudinal cracking; Numerical analysis; Widened slab; Jointed plain concrete pavement; Finite element analysis

1. Introduction

Widened slabs have been used to mitigate transverse cracking in jointed plain concrete pavements (JPCP) because, since the development of Westergard theory, [1] it has been known that edge load compared to interior or corner loads usually produces the highest stress in JPCP. While widened slabs are usually 4.3 m (14 ft) wide and constructed for traffic lanes adjacent to passing lanes (3.7 m (12 ft) wide), lane width in widened slabs is still taken to be 3.7 m (12 ft) wide, with the extra 0.6 m (2 ft) width designated as part of the pavement shoulder. By using widened slabs, load is not applied to slab edges, so transverse cracking potential is significantly diminished, but it has been known that widened slabs increase longitudinal cracking potential in JPCP [2,3]. It has been also documented that the type of shoulder adjacent to widened slabs might have an effect on longitudinal crack potential in widened slabs [2,3].

Field investigations have been conducted for widened JPCP in Iowa at 12 identified sites, including 4 control sites and 8 sites suffering from different levels of longitudinal cracking, with the goal of identifying possible reasons for observed longitudinal cracking. Details of these field investigations can be found in another study [4] that revealed that all longitudinal cracks were found to be top-down cracks, initiated at the top surfaces of widened slabs and migrating down to the bottom surfaces of the widened slabs. Another finding of the field investigations was that longitudinal cracks started mostly from transverse joints about 0.6–1.2 m (2-4 ft) away from widened slab edges. Field investigations also revealed that sites with a tied PCC shoulder had fewer longitudinal cracks than sites with hot mix asphalt (HMA) and granular shoulders [4].

While some studies have mentioned that longitudinal cracks might occur in JPCP under certain conditions [5-8], there has been no previous study focusing solely on modeling longitudinal cracking in widened JPCP.

* Corresponding author
E-mail addresses: okaya@iastate.edu (Orhan Kaya); alex19@iastate.edu (Yang Zhang); hceylan@iastate.edu (Halil Ceylan); sunghwan@iastate.edu (Sunghwan Kim); shuoy@iastate.edu (Shuo Yang); ptaylor@iastate.edu (Peter C. Taylor); rangan@iastate.edu, kasthurirangan.g@srmap.edu.in (Kasthurirangan Gopalakrishnan).
Peer review under responsibility of Chinese Society of Pavement Engineering.

ISSN: 1996-6814 DOI: https://doi.org/10.1007/s42947-019-0034-z

ISLAB 2005, a numerical analysis software package specifically developed for rigid pavement analysis, has evolved historically, and previous versions have had other names: ILSL2, ILLI-SLAB, and ISLAB2000. The earliest version of ISLAB 2005 was ILSL2 [9], developed through by collaboration of many partners: ERES Consultants in cooperation with Michigan and Minnesota Departments of Transportation, Michigan Technical University, University of Michigan, Michigan State University, and University of Minnesota [2]. ISLAB 2005 has some advanced features that significantly assist in modeling rigid pavement systems as realistically as possible [2,8,10]. Among these features are the following capabilities:

1. Selection among various subgrade models such as Winkler, elastic solid, Pasternak, Kerr-Vlasov, and Zhemochkin-Sinitsyn-Shtaerman.
2. Analyze the effects of linear and nonlinear temperature distribution throughout the pavement thickness.
3. Model interaction between a slab and its base using three models: bonded, unbonded, and Totsky.
4. Model a portion of a pavement system with different properties and features than the other parts of the pavement system.

The objective of this paper is to conduct numerical analysis in order to:

1. Seek better understanding of critical loading cases, including both mechanical and temperature loading that increases longitudinal cracking potential in JPCP.
2. Simulate longitudinal crack initiation on transverse joints.
3. Examine shoulder design alternatives to compare different shoulder alternatives (paved shoulder (partial-depth tied PCC and HMA), and full-depth tied PCC shoulder) in terms of their contributions to mitigation of longitudinal cracking potential.

2. Numerical modeling approach

A typical Iowa widened JPCP was modeled using a six-slab setup (three widened slabs in the traffic direction and three regular slabs adjacent to the widened slabs). Model definitions used throughout this paper are shown in Fig. 1, where it can be seen that widened slabs have a width of 4.3 m (14 ft) while regular slabs have a width of 3.7 m (12 ft). The lane edge shows where the lane marking is located, typically 0.6 m (2 ft) away from the widened slab edge.

A pavement configuration with a 25.4 cm (10 in) PCC thickness, a 25.4 cm (10 in) granular base, and typical Iowa subgrade (A-6) was used. Table 1 provides details of the inputs used in the FEA model.

ISLAB 2005 FEA software has been used in this study as the main structural model for generating rigid pavement responses of Iowa widened JPCP under mechanical and temperature loading. ISLAB 2005 discretizes modeled slabs into meshes and nodes. FEA uses a fine mesh size (nominal element size of 15.2 cm (6 in)). At the completion of FEA, ISLAB produces an output file in "txt" format for each FEA scenario considered (630 txt files in total for the single axle load cases introduced later in this paper), representing stress (in x direction, y direction, principal stress and von mises stress) and deflection results for each nodal value. These output files require post-processing so that critical pavement responses for each FEA scenario can be calculated and extracted.

A post-processing scheme using Microsoft Excel VBA (Visual Basic for Applications) and MATLAB (version 9.3.0.713579 [R2017b]) was developed. It combines all output files, calculates and summarizes critical pavement responses for each FEA scenario, and presents them in a summary worksheet. The post-processing steps are as the following: (1) The output files are initially transferred into a master Excel spreadsheet using Microsoft Excel VBA; (2) Using MATLAB, critical pavement responses are calculated, extracted, and written into a summary Excel spreadsheet. Critical stresses summarized are as follows: maximum top and bottom (top and bottom of slab) tensile stresses in x and y directions, maximum top and bottom principal and von mises stresses and maximum deflections.

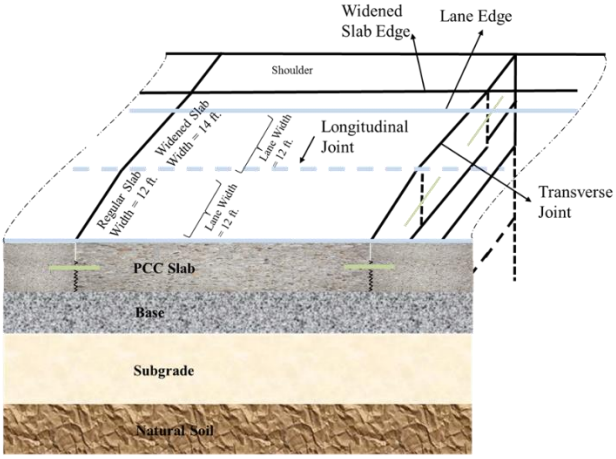

Fig. 1. FEA model definitions.

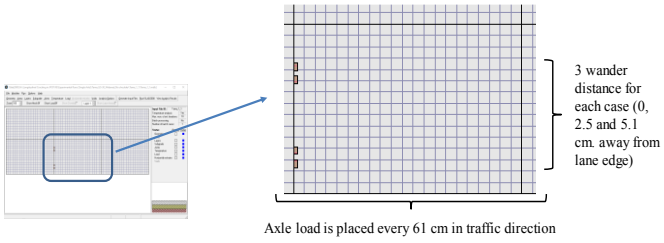

Fig. 2. Single-axle load cases.

3. Single axle load simulations

Several FEA models were developed for (1) mechanical-load-only cases and (2) combined temperature and mechanical load cases. To simulate mechanical load, a single axle with dual wheels carrying a total load of 9.1 metric-tons (20,000 lbs.) was used. To simulate temperature loads, 21 different temperature cases were used with temperature gradients from -0.3 to 0.3 (°C/cm) in increments of 0.03 (°C/cm) (Table 1). A single axle load was placed every 60 cm (2 ft) in the traffic direction and three wander distances (0, 30, and 60 cm (0, 1, and 2 ft away from lane edge)). A total of 630 FEA scenarios were modeled in ISLAB 2005 for single-axle load simulations (Fig. 2).

ISLAB 2005 produces tensile stress results in the x and y directions (x direction is perpendicular to the traffic direction, y direction is the traffic direction). Tensile stress results on slab surface (top) in the x and y directions as well as deflection results were first analyzed to determine which tensile stress type (in the x or y direction) is the critical tensile stress type for producing

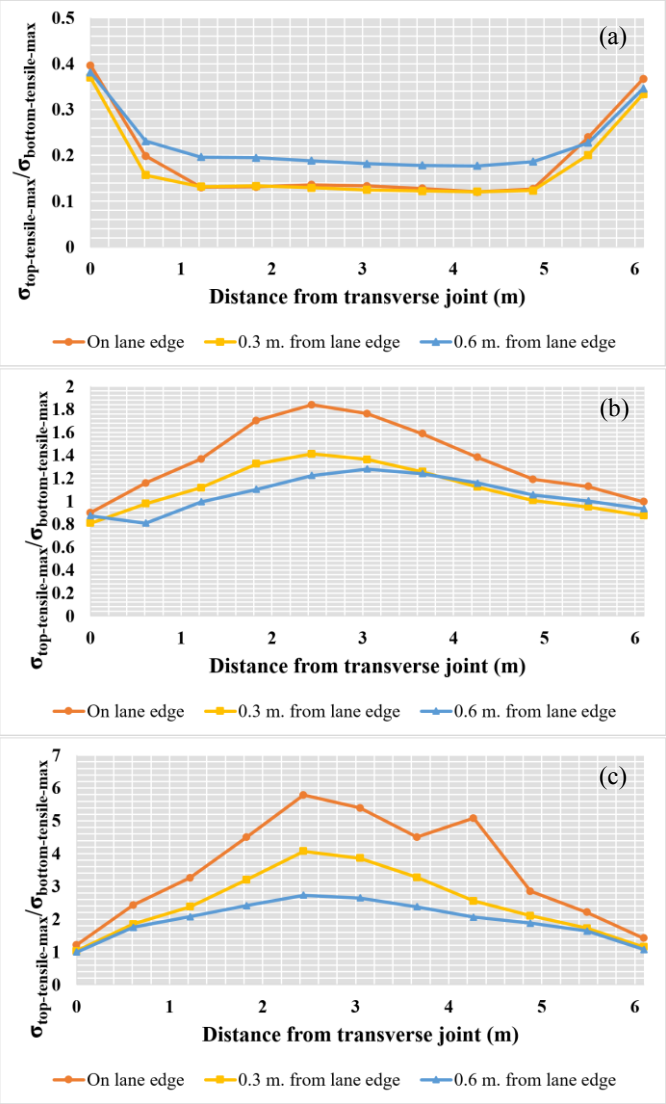

Fig. 3. Top and bottom tensile stress ratio distribution for single axle mechanical load combined with three different temperature load scenarios; (a) ΔT= 0°C (0°F), (b) - 5.5°C (-10°F), and (c) ΔT= -11°C (-20°F) applied on various locations in both traffic and wander directions.

longitudinal cracking. Based on analysis results of various mechanical and temperature loading scenarios, tensile stresses in the x direction were found to be the critical stresses for longitudinal cracking because they are tensile stresses perpendicular to the traffic direction. The tensile stresses in the y direction would be critical for transverse cracking because they are tensile stresses parallel to the traffic direction. In this study, tensile stresses in the x direction were used as critical tensile stresses to characterize longitudinal cracking.

3.1. Single axle load simulation results

Fig. 3 shows the top-to-bottom tensile stress ratio distribution when single-axle mechanical loads are applied at various locations in both traffic (distance from transverse joints) and wander directions for three different temperature load scenarios; (a) no temperature load (ΔT= 0°C (0°F)), (b) temperature difference

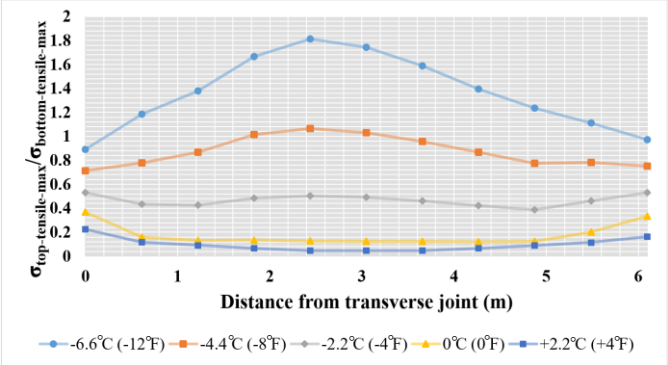

Fig. 4. Top-to-bottom tensile stress ratio distribution for various combined mechanical and temperature load cases.

between bottom and top of slab of 5.5°C (10°F) (ΔT= top-bottom= -5.5°C (-10°F)), and (c) temperature load with ΔT= -11°C (-20°F). The notation of top-to-bottom tensile stress ratio is used throughout this paper to evaluate for which loading scenarios potential longitudinal cracking might be top-down cracking. Cases where the top-to-bottom ratio is higher than 1 represent those cases where potential longitudinal cracking would be top-down. As discussed earlier, field investigations revealed that all observed longitudinal cracks were top-down cracks. As seen in Fig. 3(a), higher top-to-bottom tensile stress ratio values were observed when a single-axle mechanical load was applied on transverse joints with no temperature loading. While there was no significant difference in top-to-bottom tensile stress ratio results for different wander distances, a slightly higher top-to-bottom stress ratio was observed when the outer wheel of the single axle was placed 0.3 m (1ft) away from the lane edge, compared to cases when the outer wheel of the single axle was placed on the lane edge and 0.6 m (2 ft) away from the lane edge. (Fig. 3(a)). On the other hand, as shown in Fig. 3(b), a very high top-to-bottom tensile stress ratio (as high as 1.8) was observed when combined mechanical and temperature load (ΔT= -5.5°C (-10°F)) was applied around mid-slab. Although there was no significant difference in the top-to-bottom tensile stress ratio results for different wander distances, when the outer wheel of the single axle was placed on the lane edge, a slightly higher top-to-bottom stress ratio was observed compared to when the outer wheel of the single axle was placed 0.3 m (1 ft) and 0.6 m (2 ft) away from the lane edge. (Fig. 3(b)). Similarly, as shown in Fig. 3(c), a very high top-to-bottom tensile stress ratio (as high as 5.8) was observed when combined mechanical and temperature load (ΔT= -11°C (-20°F)) was applied around mid-slab.

Fig. 4 shows the top-to-bottom tensile stress ratio distribution when various combined mechanical and temperature load scenarios are applied at lane edge and various locations in the traffic direction. As can be seen in Fig. 4, as the negative temperature gradient increases, higher top-to-bottom tensile stress ratio values are observed around mid-slab.

In summary, various FEA cases using single-axle loads were examined, and the effects of combined mechanical and temperature loads on tensile stress development on slab surfaces were investigated. Effects of load and wander patterns on tensile stress development on slab surfaces also became better understood. It was determined that the critical tensile stress locations are as follows:

1. Close to transverse joint for mechanical load only.
2. Close to mid-slab surface as temperature gradient increases.

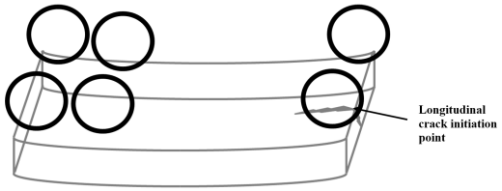

Fig. 5. Failure mechanism for longitudinal cracking from field investigation.

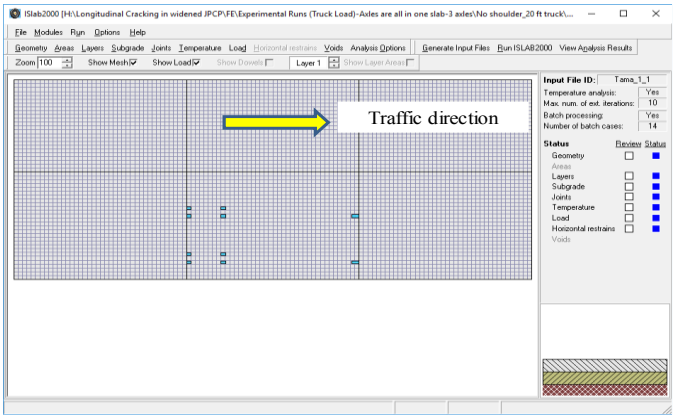

Fig. 6. Three-axle truck with 6.1 m (20 ft) axle spacing – discretized truck load.

In combined mechanical and temperature loading cases, as the negative temperature gradient increased, higher top-to-bottom tensile stress ratio values were observed around mid-slab. Further analysis was conducted for applied truck loads.

4. Truck load simulations

Based on the field investigations described in the previous sections of this paper, the failure mechanisms of Iowa JPCP widened slabs with respect to longitudinal cracking include longitudinal cracks initiated from transverse joints as top-down cracking, mainly on the widened traffic lane and about 0.6 to 1.2 m (2 to 4 ft) away from the slab edge (Fig. 5).

In this section, several truck axle-load and spacing configurations are investigated to evaluate the effects of axle load and spacing configurations on longitudinal cracking, and the critical axle load and spacing configuration resulting in the highest longitudinal cracking potential is also identified.

Mechanical loads for single-axle and tandem axles were applied at levels of 9.1 and 15.4 metric-tons (20 and 34 kips), respectively, based on Federal Highway Administration (FHWA) [11] and Iowa DOT guidelines [12].

Two what-if scenarios including three- and four-axle and spacing configurations were investigated:

1. Three-axle truck with 6.1 m (20 ft) axle spacing placed on a single slab.
2. Four-axle truck with 7.0 m (23 ft) axle spacing with both axle groups partially placed on adjacent slabs.

4.1. Three-axle truck with 6.1 m (20 ft) axle spacing placed on a single slab

In this loading scenario, a truck with both a single axle and a tandem axle is used as a truckload (Class 6 based on FHWA truck classification [11] (Fig. 6), with single and tandem axles applying mechanical loads of 9.1 and 15.4 metric-tons (20 and 34 kips), respectively, on the pavement system (Fig. 6). The 6.1 m (20 ft) figure was selected as the axle spacing, i.e., the distance between

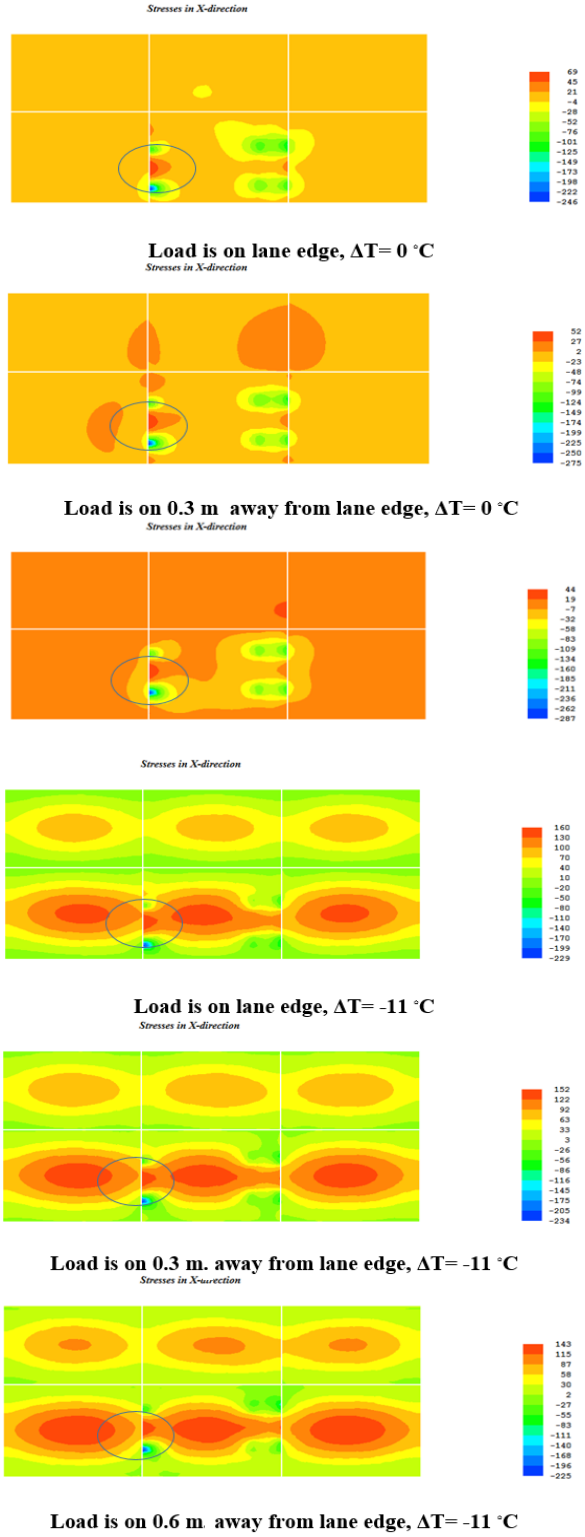

Fig. 7. Three-axle truck with 6.1 m (20 ft) axle spacing – top tensile stress distribution for three wander distances and two temperature load cases.

the center of the rear axle of the tandem axle and that of the the single axle, so that both single and tandem axle loads are placed on two transverse joints of the widened slabs (JPCP has a joint spacing of 6.1 m (20 ft)) (Fig. 6). Five different wander distances were tested (0, 15, 30, 45, and 60 cm (0. 0.5, 1, 1.5, and 2 ft) away from the lane edge (Table 1).

Fig. 7 shows the top tensile stress distribution when a truck load is applied at three wander distances (on lane edge and 0.3 and 0.6 m (1 and 2 ft) away from lane edge for two temperature load cases (only mechanical load (ΔT= 0°C) and combined mechanical and temperature load (ΔT= -11°C (-20°F)). As seen in Fig. 7, very high top tensile stresses can be observed starting from transverse joints, representing greater potential for longitudinal crack initiation starting from the transverse joint of the slab surface.

Fig. 8 shows the top-to-bottom tensile stress ratio distribution when various combined mechanical and temperature load scenarios are applied at various wander distances (0 to 0.6 m (0 to 2 ft)). As can be seen in Fig. 8, as the negative temperature gradient increases, the top-to-bottom tensile stress ratios also increase. Moreover, as truck load is placed closer to the lane edge (wander distance decreases) the top-to-bottom tensile stress ratios increase.

Fig. 9 shows the top tensile stress distribution when various combined mechanical and temperature load scenarios are applied at various wander distances (0 to 0.6 m (0 to 2 ft)). The top tensile stress distribution exhibits a similar trend as the top-to-bottom tensile stress ratios; as the negative temperature gradient increases, the top tensile stresses also increase; and as the truck load is placed closer to the lane edge, the top tensile stresses also increase.

Results based on this loading scenario can be summarized as follows.

1. A higher negative temperature gradient produced higher top-to-bottom tensile stress ratios.
2. Higher top and bottom tensile stress ratio values were observed close to the lane edge, (highest right on the lane edge).
3. For high temperature load cases, the critical tensile stress location was identified as the transverse slab joint.

4.2. Four-axle truck with 7.0 m (23 ft) axle spacing with both axle groups partially placed on adjacent slabs

It was concluded from the three-axle truck case that when axle loads are placed on adjacent slabs, tensile stresses are transferred to a critical slab (the slab between adjacent slabs), causing very high tensile stress to accumulate around the top surface of the critical slab surface close to the transverse edge. This is especially true for high negative temperature gradient cases (when slabs curl up) where the center of axle loads are placed close to the transverse edges (Fig. 10). In that case, the top tensile stresses on the transverse edges of the adjacent slabs are transferred to the critical slabs and very high top tensile stresses are observed around the transverse joints of the critical slabs (Fig. 10). In this loading scenario, a two tandem axles (four-axle) configuration with a 7.0 m (23 ft) axle spacing is used, and the centers of the axle loads are placed close to the transverse edges. Each tandem axle applies a total mechanical load of 15.4 metric-tons (34 kips) (Fig. 11). Use of two tandem axles as mechanical load simulates the two axles of a Class 9 truck [11] (18-wheeler), the most commonly-used truck type [2]. The objective of this analysis was to determine the critical loading scenario producing the highest top-to-bottom tensile stress ratios.

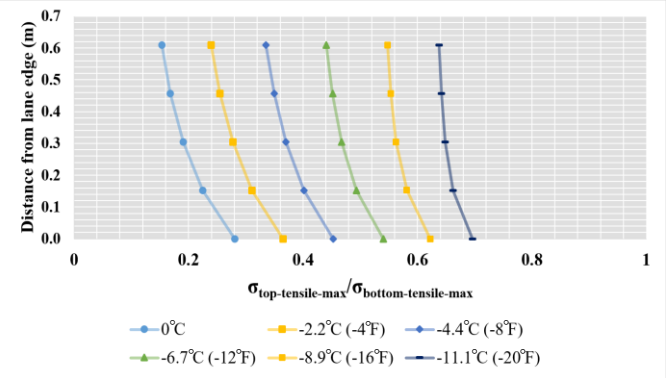

Fig. 8. Three-axle truck with 6.1 m (20 ft) axle spacing – top-to-bottom tensile stress ratio distribution.

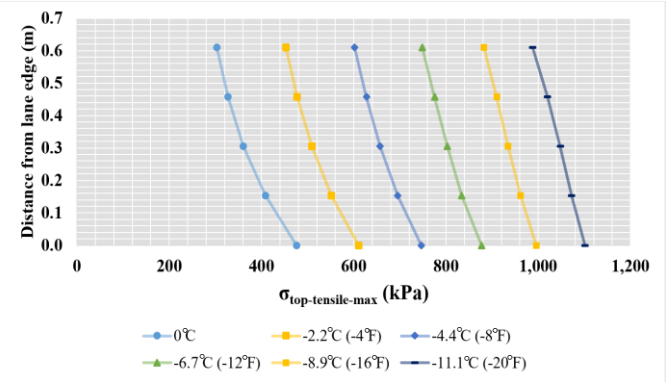

Fig. 9. Three-axle truck with 6.1 m (20 ft) axle spacing – top tensile stress distribution.

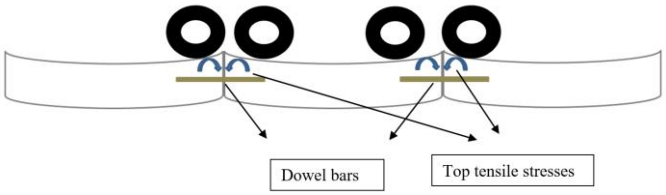

Fig. 10. Top tensile stress transfer mechanism in four-axle truck.

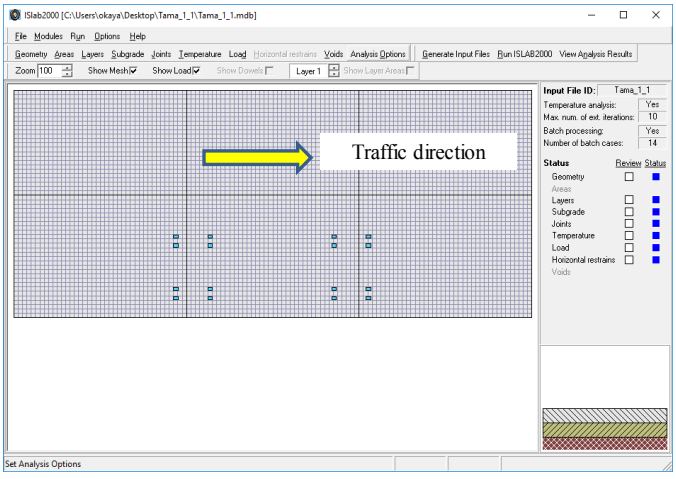

Fig. 11. Four-axle truck – discretized truck load.

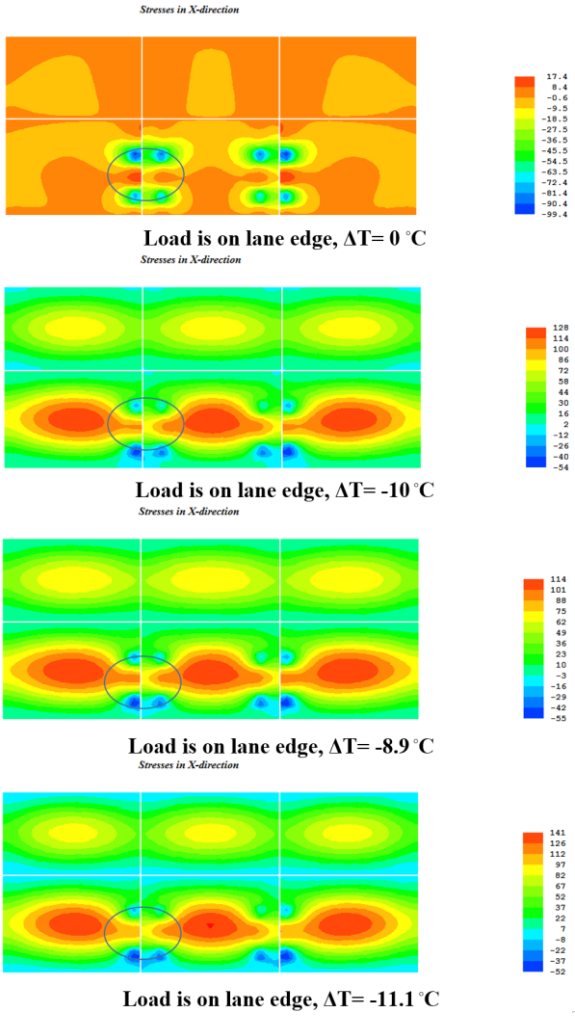

Fig. 12. Four-axle truck – top tensile stress distribution for four temperature load cases.

Fig. 12 shows the top tensile stress distribution when the truck load is applied on the lane edge for four temperature-load cases, both including mechanical load only and combined mechanical and temperature load (ΔT= -8.9°C (-16°F), -10°C (-18°F) and -11.1°C (-20°F)). As can be seen in Fig. 12, very high top-to-bottom tensile stress ratios, as high as 3.2, are observed close to the transverse edge.

Fig. 13 shows the top-to-bottom tensile stress ratio distributions when various combined mechanical and temperature load scenarios are applied at various wander distances (0 to 0.6 m (0 to 2 ft)). As can be seen in Fig. 13, as the temperature difference between top and bottom of the slab increases, top-to-bottom tensile stress ratios also increase to as high as 3.2.

Fig. 14 shows top tensile stress distributions when various combined mechanical and temperature load scenarios are applied at the lane edge. The top tensile stress distribution shows a similar trend as the top-to-bottom tensile stress ratios, i.e., as the negative temperature gradient increases, the top tensile stresses also increase.

Fig. 15 shows comparisons of tensile stress distributions between a three-axle truck and a four-axle truck for two loading scenarios: mechanical load only and combined mechanical and temperature load (ΔT= -11.1°C (-20°F)). As can be seen in Fig. 15, similar top tensile stress results were observed in both cases, except that the

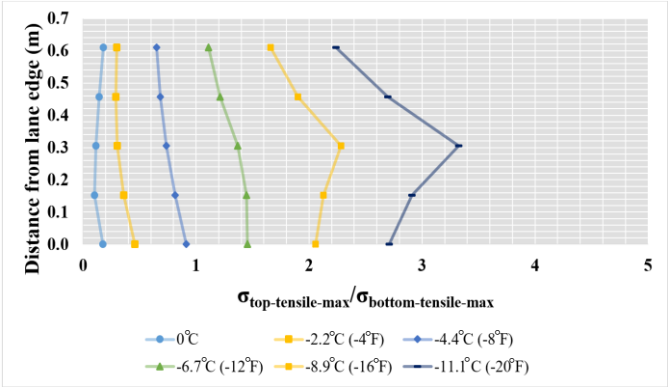

Fig. 13. Four-axle truck – top-to-bottom tensile stress ratio distribution.

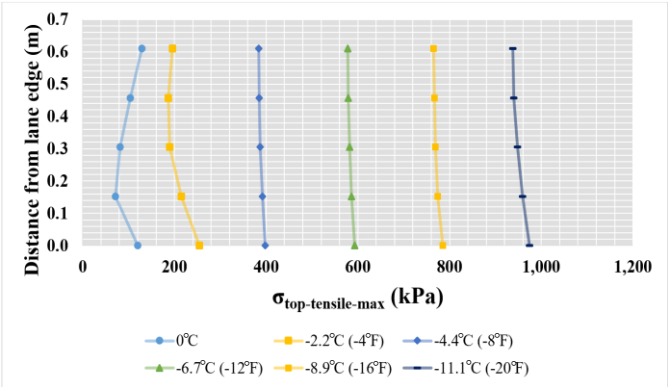

Fig. 14. Four-axle truck – top tensile stress distribution.

truck with a four-axle transfer case produced a significantly higher (as high as 2.7) top-to-bottom tensile stress ratio.

4.3. Truck load simulations - summary of findings

The top-down longitudinal cracking potential for JPCP with widened slabs was satisfactorily demonstrated using several truckload configurations. The key findings were as follows:

1. Longitudinal cracking initiatiates from the transverse joints between the lane edge and wheel path.
2. Although both three- and four-axle configurations produced similarly high tensile stresses, a truck with a four-axle case produced significantly higher (as high as 2.7) top-to-bottom tensile stress ratios, so the four-axle truck load configuration was identified as the critical loading scenario.
3. A higher negative temperature gradient between the top and bottom of the slab produced higher top-to-bottom tensile stress ratios and, in turn, led to greater longitudinal cracking potential.

5. Shoulder design alternatives simulations

Three shoulder design alternatives were compared for both widened (4.3 m (14 ft) wide) and regular size (3.7 m (12 ft) wide) slabs: Partial-depth tied PCC, HMA (paved shoulder alternates), and full-depth tied PCC shoulder (Fig. 16). These shoulder types were modeled based on the Iowa DOT's typical design details [13] (Fig. 16).

Shoulder design alternatives were compared for the following cases:

Tied PCC shoulder using:

1. Regular slabs (3.7 m (12 ft) wide) with a full-depth tied PCC shoulder; shoulder thickness is the same as regular slab thickness (i.e., 25.4 cm (10 in)).
2. Widened slabs (4.3 m (14 ft) wide) with a partial-depth tied PCC shoulder alternative; shoulder thickness is less than regular slab thickness (i.e., 17.8 cm (7 in)).

HMA shoulder using:

1. Regular slabs (3.7 m (12 ft) wide) with an HMA shoulder alternative; shoulder thickness is less than regular slab thickness (i.e., 20.3 cm (8 in)).
2. Widened slabs (4.3 m (14 ft) wide) with an HMA shoulder alternative; shoulder thickness is less than regular slab thickness (i.e., 20.3 cm (8 in)).

Table 1
FEA model inputs.

Slab size and properties	
Slab size in traffic direction (m)	6.1
Slab size in transverse direction (m) - Regular slab	3.7
Slab size in transverse direction (ft) - Widened slab	4.3
Finite element mesh size (cm)	15.2
Slab thickness (cm)	25.4
Elastic modulus (MPa)	27,580
Poisson ratio	0.2
Coefficient of thermal expansion (CTE) (1/°C)	8.8E-06
Unit weight (kg/m^3)	2,400
Granular base size and properties	
Base thickness (cm)	25.4
Elastic modulus (MPa)	241
Poisson ratio	0.35
CTE (1/°C) of granular material	9.0E-06
Unit weight (kg/m^3)	2,038
Subgrade properties	
k (MPa/mm)	0.044
Mechanical and temperature loading	
Load level (metric-tons)	9.1 (single axle), 15.4 (tandem axle)
Tire pressure (kPa)	827
Load location in traffic Direction	Every 60 cm. (2 ft) for single axle load cases 0, 30 and 60 cm (0, 1 and 2 ft) away from lane edge (for single axle load cases)
Wander pattern	0, 15, 30, 45 and 60 cm. (0. 0.5, 1, 1.5 and 2 ft) away from lane edge (for truck load cases)
Long term load transfer efficiency (LTE) (%)	70
Temperature gradient (°C/cm)	-0.3 to 0.3 with an increment of 0.03 (-2 to 2°F/in with an increment of 0.2)

The critical load configurations found in the truckload simulations were used for mechanical load configurations. Five different wander distances were investigated: 0, 15, 30, 45, and 60 cm (0. 0.5, 1, 1.5, and 2 ft), respectively, away from the lane edge for widened slabs, and at the slab edge itself for regular slab sizes. Other model inputs were the same as for the truckload simulations (Table 1).

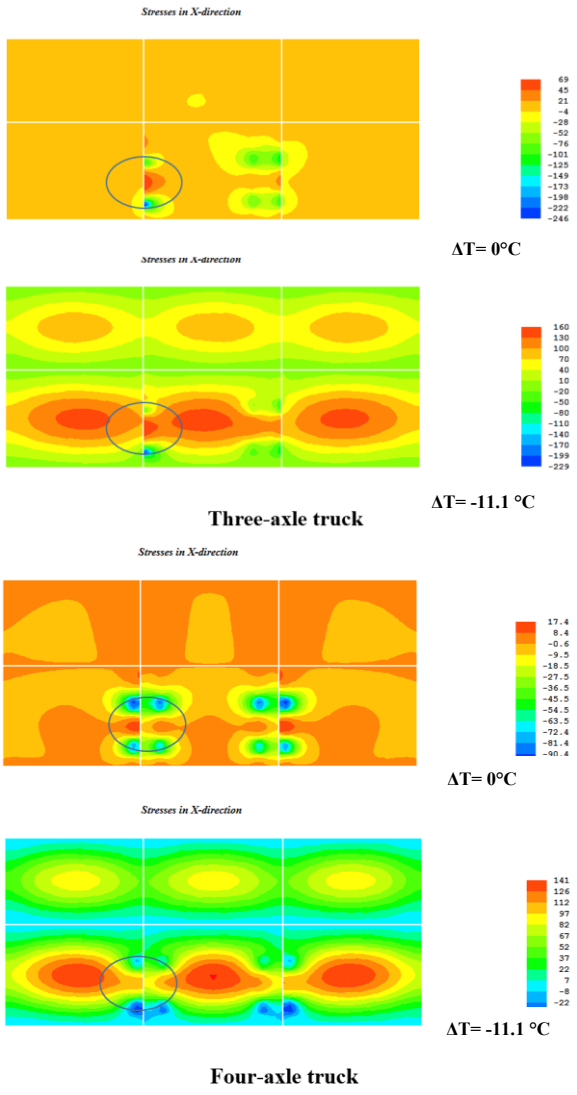

Fig. 15. Comparisons of tensile stress distributions between a three-axle truck and a four-axle truck.

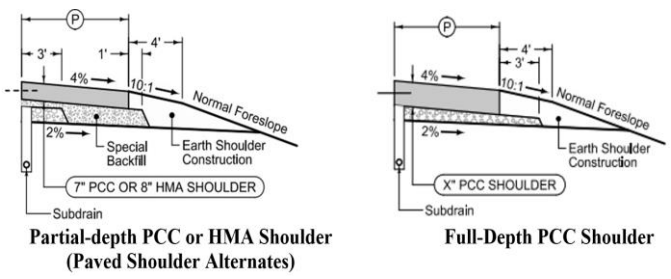

Fig. 16. Shoulder design alternatives.

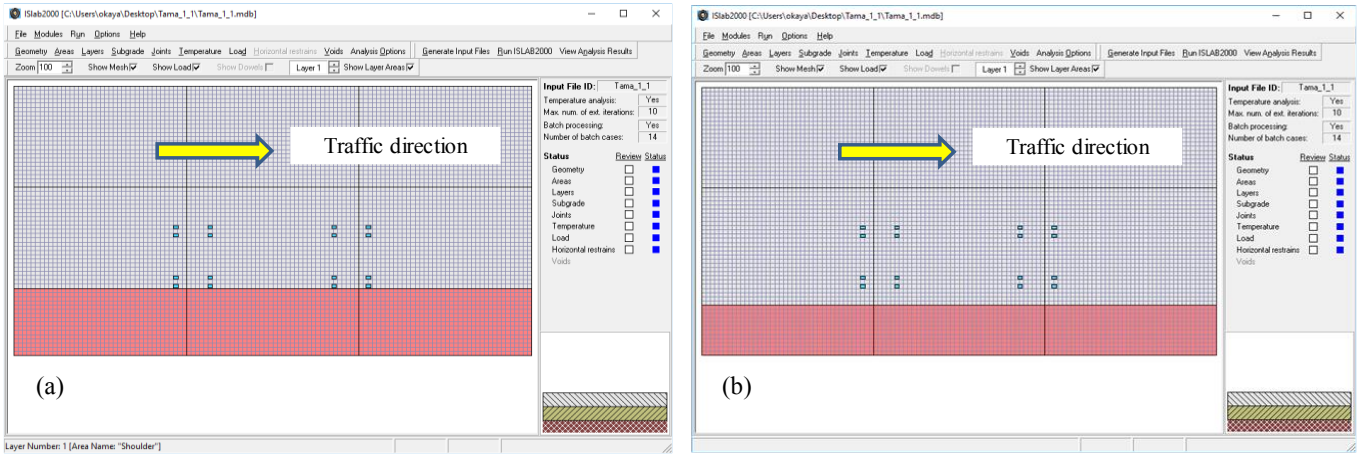

Fig. 17. Widened and regular size slabs with shoulder design alternatives (a) regular size slabs with shoulder design alternatives and (b) widened size slabs with shoulder design alternatives.

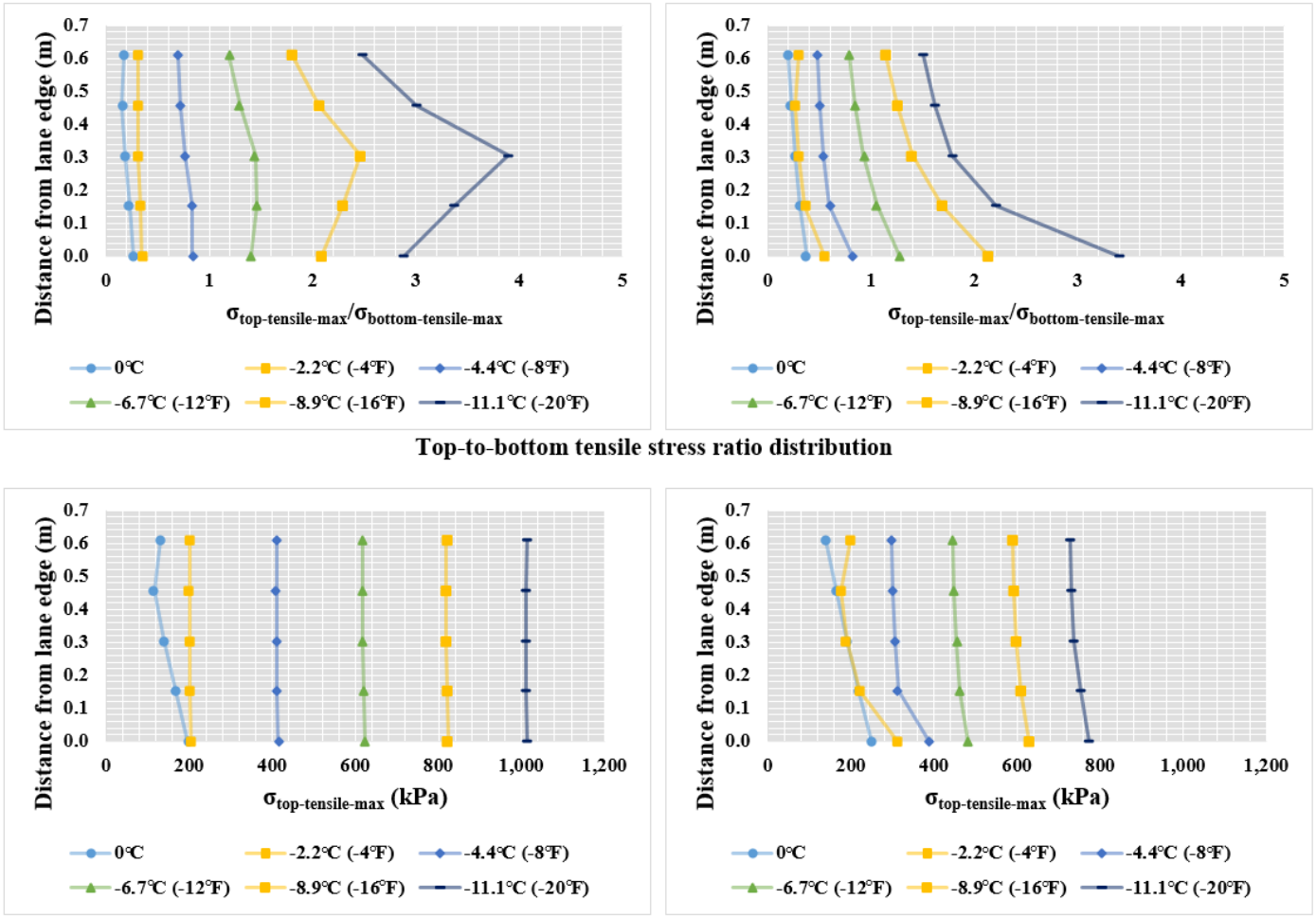

Fig. 18. Top-to-bottom tensile stress ratio and top tensile stress comparisons between a widened slab with partial-depth tied PCC shoulder and a regular slab with full-depth tied PCC shoulder.

Fig. 17 shows the discretized models for the shoulder design alternatives. The widened slab (4.3 m (14 ft) wide) had a 0.6 m (2 ft) extended width compared to a regular slab size (3.7 m (12 ft) wide). An alternative shoulder width was selected to ensure that the total width, including both slab and shoulder, would constitute a 6.1 m (20 ft) widened slab with a 1.8 m (6 ft) shoulder and a regular slab width with a 2.4 m (8 ft) shoulder.

5.1. Tied PCC shoulder

In this alternative shoulder scenario, two cases were compared:

1. A regular slab (3.7 m (12 ft) wide) with a full-depth tied PCC shoulder in which the shoulder thickness has the same thickness as that of regular slab (i.e., 25.4 cm (10 in)).
2. A widened slab (4.3 m (14 ft) wide) with a partial-depth tied PCC shoulder alternative in which the shoulder thickness is less than that of a regular slab thickness (i.e., 17.8 cm (7 in)).

Fig. 18 compares the top-to-bottom tensile stress ratios and top tensile stress distributions between a widened slab with a partial-depth tied PCC shoulder and a regular slab with a full-depth tied PCC shoulder. As can be seen in Fig. 18, both higher top-to-bottom tensile stress ratios and top tensile stresses were observed for a widened slab with a partial-depth tied PCC shoulder compared to those for a regular slab with a full-depth tied PCC shoulder. In terms of longitudinal cracking potential, the mid-slab edge was found to be critical when regular slabs were used while the transverse joint edge was found to be critical when widened slabs were used.

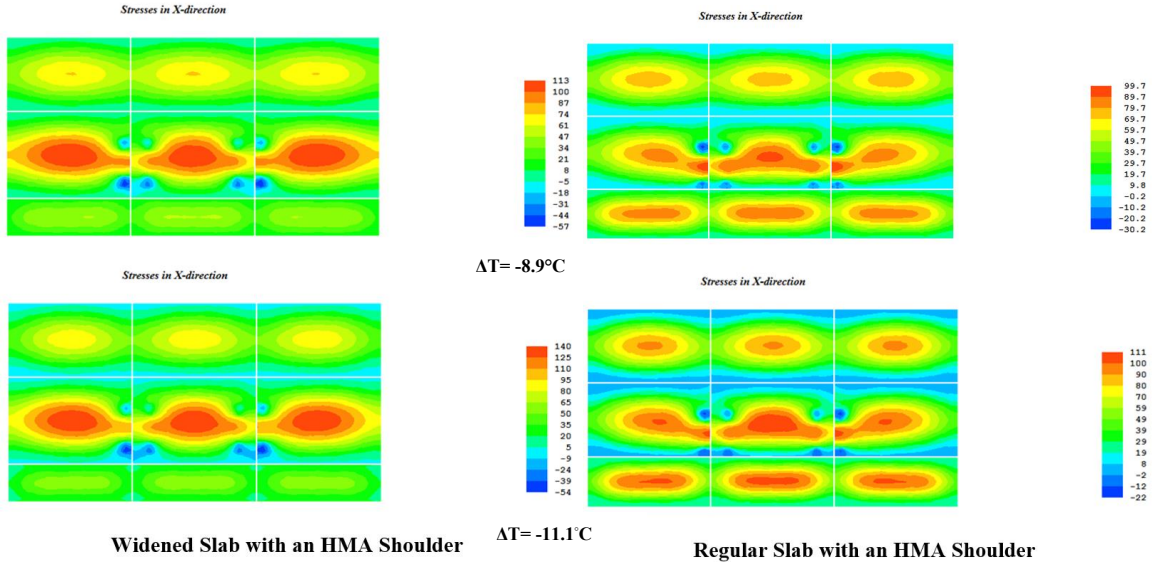

Fig. 19. Comparisons of tensile stress distributions between widened and regular slabs with an HMA shoulder.

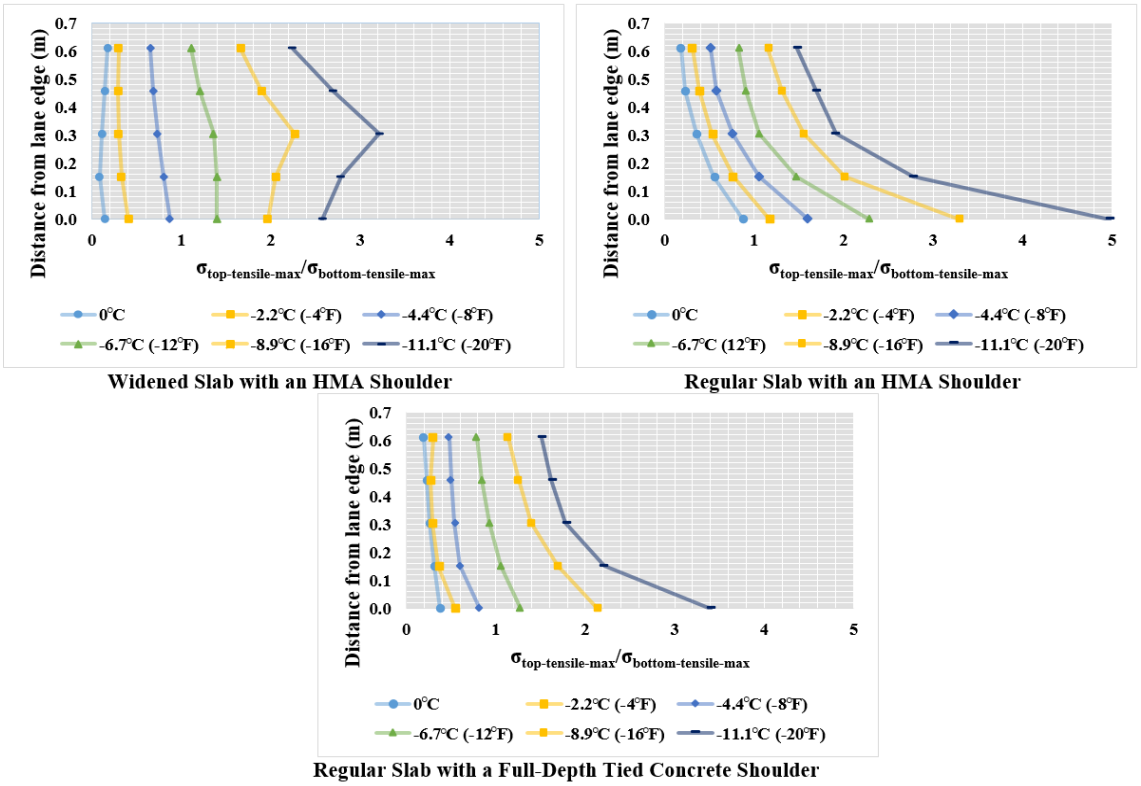

Fig. 20. Top-to-bottom tensile stress ratio comparisons between widened slab with an HMA shoulder, regular slab an HMA shoulder and regular slab with a full-depth tied PCC shoulder.

5.2. HMA shoulder

In this alternative scenario, two cases were compared:

1. A regular slab (3.7 m (12 ft) wide) with an HMA shoulder alternative in which the shoulder thickness is less than that of a regular slab (i.e., 20.3 cm (8 in)).
2. A widened slab (4.3 m (14 ft) wide) with an HMA shoulder alternative in which the shoulder thickness is less than that of a regular slab (i.e., 20.3 cm (8 in)).

Load transfer between a widened or regular slab and an HMA shoulder was modeled in such a way that there is load transfer only between granular bases of the widened or regular size slabs and HMA shoulders. This load transfer is modeled by assigning a load transfer efficiency (LTE) value of 10% between slabs and HMA shoulders based on a recommendation from an NCHRP report [2].

Fig. 19 shows comparisons of tensile stress distributions between widened and regular size slabs with an HMA shoulder for two loading scenarios: combined mechanical and temperature load ((ΔT= -11.1°C (-20°F)) and ((ΔT= -8.9°C (-16°F)). As can be seen in Fig. 19, higher top tensile stress results were observed when widened slabs are used with an HMA shoulder compared to when regular slabs are used with an HMA shoulder.

Fig. 20 compares the top-to-bottom tensile stress ratios between a widened slab with an HMA shoulder, a regular slab with an HMA shoulder, and a regular slab with a full-depth tied PCC shoulder. As can be seen in Fig. 20, among the cases presented the highest top-to-bottom tensile stress ratio was observed for the regular slab with an HMA shoulder.

5.3. Shoulder design alternatives simulations - summary of findings

A higher (1) top-to-bottom tensile stress ratio and (2) top tensile stress was observed for a widened slab (4.3 m (14 ft) wide) with a partial-depth tied PCC shoulder alternative compared to a regular size slab (3.7 m (12 ft) wide) with a full-depth tied PCC shoulder. A higher top-to-bottom tensile stress ratio was observed for a regular size slab (3.7 m (12 ft) wide) with an HMA shoulder compared to a widened slab (4.3 m (14 ft) wide) with an HMA shoulder. On the other hand, higher tensile stresses were observed for a widened slab (4.3 m (14 ft) wide) with an HMA shoulder compared those for a regular size slab (3.7 m (12 ft) wide) with an HMA shoulder. Compared to the use of a widened slab, the use of a regular size slab was found to be beneficial in mitigating longitudinal cracking at the cost of increasing transverse cracking potential.

6. Conclusions and discussion

One of the objectives of this paper was to understand longitudinal cracking mechanisms and to evaluate longitudinal cracking potential of widened JPCP through numerical analysis. Initially, both tensile stress results on the slab surface (top) in the x and y directions and deflection results were analyzed through single-axle load simulation to determine which tensile stress type (in the x or y direction) is critical in producing longitudinal cracking. Based on the single-axle load simulation results, tensile stresses in the x direction were found to be the critical ones with respect to producing longitudinal cracking. Although much useful information for characterizing critical load locations for longitudinal cracking can be found through single-axle load simulation, truck load configurations were thought to better simulate the critical loading scenario associated with the highest longitudinal cracking potential, so three and four-axle truck loads were investigated. A truck with a four-axle configuration with the center of its axle loads placed close to transverse edges was identified as the critical loading scenario, because when axle loads were placed on adjacent slabs, tensile stresses were transferred to the critical slab, resulting in very high tensile stress accumulation around the top surface of the critical slab close to the transverse edge. This is especially true for high negative temperature gradient cases (when slabs curl up) where the center of the axle loads is placed close to the transverse edges of an adjacent slab. In that case, the top tensile stresses on the transverse edges of the adjacent slabs are transferred to the critical slabs and extremely high top tensile stresses are observed around the transverse joints of the critical slabs. This finding satisfactorily explains the longitudinal crack initiation at the transverse joints and top slab surface observed in the field investigations.

Another objective of this paper was to compare different shoulder types when used adjacent to either a widened (4.3 m (14 ft) wide) or a regular size (3.7 m (12 ft) wide) slab in terms of their effects in mitigating longitudinal cracking. Initially, widened slabs with a partial-depth tied PCC shoulder alternative were compared with regular slabs with a full-depth tied PCC shoulder alternative, and it was found that higher (1) top-to-bottom tensile stress ratio and (2) top tensile stress were observed when widened slabs with a partial-depth tied PCC shoulder were used, compared to when regular slabs with a full-depth tied PCC shoulder were used. Higher top-to-bottom tensile stress ratio and top tensile stresses are related to higher longitudinal cracking potential, possibly because even though widened slabs can be used to mitigate transverse cracking, they might increase longitudinal cracking potential. This characteristic of widened slabs does not change much even if when they are used with a partial-depth tied PCC shoulder.

In this paper, widened slabs (4.3 m (14 ft) wide) with an HMA shoulder alternative were also compared to regular slabs (3.7 m (12 ft) wide) with an HMA shoulder alternative in terms of their effect on mitigating longitudinal cracking. A higher top-to-bottom tensile stress ratio was observed when regular slabs (3.7 m (12 ft) wide) with an HMA shoulder were used compared to the situation of widened slabs (4.3 m (14 ft) wide) with an HMA shoulder. The difference between an HMA shoulder alternative and a tied PCC shoulder alternative is that the HMA shoulder is not tied to widened or regular slabs so there is no load transfer between a slab and the HMA shoulder, and a LTE of only 10% is defined between the shoulder and slab bases, explaining why the effect of an HMA shoulder on top tensile stress accumulation in widened or regular slabs is minimal. In short, widened slabs or regular slabs with HMA shoulders demonstrate similar behavior when there is no shoulder used with them in terms of their effect on longitudinal cracking potential.

7. Recommendations

Recommendations of this study for mitigating longitudinal cracking in widened JPCP can be summarized follows:

1. Longitudinal cracks are mainly in the traffic lane and about 0.3-0.6 m (2~4 ft) away from slab edge
2. Shorter joint spacing can result in lower curling and warping and also can lead to less chance for longitudinal cracking as well
3. Most longitudinal cracks observed start from slab transverse joints

4. Since dowel bars can restrain vertical deflection at joints, so proper dowel bar installation will help mitigate longitudinal cracking
5. A tied PCC shoulder design option can perform better than other shoulder design options (HMA and granular) in terms of longitudinal crack potential in widened JPCP.

Acknowledgements

The authors would like to thank the Iowa Department of Transportation (DOT) for sponsoring this research. The project's Technical Advisory Committee (TAC) members, Ben Behnami, Chris Brakke, Vanessa Goetz, Todd Hanson, Kevin Merryman and Jason Omundson of Iowa DOT; Jacob Thorius of Washington County, Iowa; Greg Mulder of Iowa Concrete Paving Association (ICPA); Gordon Smith of ISU CP Tech Center and John Cunningham of Snyder & Associates, Inc. are gratefully acknowledged for their guidance. The contents of this paper reflect the views of the authors who are responsible for the facts and accuracy of the data presented within. The contents do not necessarily reflect the official views and policies of the Iowa DOT. This paper does not constitute a standard, specification, or regulation.

References

[1] R. Horonjeff, E. Bone, H.M. Westergaard, New Formulas For Stresses in Concrete Pavements of Airfields. Transactions, Discussion. Transactions of The American Society of Civil Engineers 113 (1948) 440-444.

[2] NCHRP, Guide for Mechanistic-Empirical Design of New and Rehabilitated Pavement Structures, Champaign, IL., 2003.

[3] R.E. Lederle, Development of a Longitudinal Cracking Fatigue Damage Model for Jointed Plain Concrete Pavements Using the Principles of Similarity, University of Minnesota, MN., 2014.

[4] H. Ceylan, S. Kim, Y. Zhang, S. Yang, O. Kaya, K. Gopalakrishnan and P. Taylor, Prevention of Longitudinal Cracking in Iowa Widened Concrete Pavement. Final Report, IHRB Project TR-700. Iowa State University, 2018.

[5] J.E. Hiller, J.R. Roesler, Determination of Critical Concrete Pavement Fatigue Damage Locations Using Influence Lines, J. Transp. Eng. 131 (8) (2005) 599-607.

[6] A.C. Heath, J.R. Roesler, J.T. Harvey, Modeling Longitudinal, Corner and Transverse Cracking in Jointed Concrete Pavements. Int. J. Pave. Eng. 4 (1) (2003) 51–58.

[7] J.E. Hiller, J.R. Roesler, Transverse Joint Analysis for use in Mechanistic-Empirical Design of Rigid Pavements, Transp. Res. Rec. 1089 (2002) 42–51.

[8] S. Kim, H. Ceylan and K. Gopalakrishnan, Finite Element Modelling of Environmental Effects on Rigid Pavement Deformation, Frontiers Struc. Civ. Eng. J. 8 (2) (2014) 101-114.

[9] L. Khazanovich, Structural Analysis of Multi-Layered Concrete Pavement Systems, (Ph.D. Thesis), University of Illinois, Urbana, IL., 1994.

[10] F. Mu, J. Vandenbossche, Evaluation of the Approach used for Modeling the Base under Jointed Plain Concrete Pavements in the AASHTO Pavement ME Design Guide, Int. J. Pave. Res. Tech. 9 (4) (2016) 264-269.

[11] FHWA, Compilation of Existing State Truck Size and Weight Limit Laws, Washington DC., 2015.

[12] Iowa DOT, Iowa Truck Information Guide, July 2017-July 2018 Edition, 2018.

[13] Iowa DOT, Iowa DOT Office of Design, Road Design Details - Typical Components, 2018.